Int. J. Heat Mass Transfer. Vol. 16, pp. 337–346. Pergamon Press 1973. Printed in Great Britain

DROP SIZE DISTRIBUTIONS AND HEAT TRANSFER IN DROPWISE CONDENSATION

CLARK GRAHAM

Naval Ship Engineering Center. Navsec 6103. Dept. of the Navy
Center Building. Prince George Center. Hyattsville. Md. 20782. U.S.A.

and

PETER GRIFFITH

Dept. of Mechanical Engineering. Massachusetts Institute of Technology. Cambridge. Mass. 02139. U.S.A.

(*Received* 31 *January* 1972)

Abstract— Drop distributions have been determined at atmospheric and low pressure for dropwise condensation on a smooth vertical copper surface promoted with di-octadecyl disulphide. Nucleation site densities of 200×10^6 sites/cm^2 were found. Significantly larger drop populations were found at atmospheric pressures than low pressures.

By means of a heat transfer theory it was found that at atmospheric pressure. drop conduction was the limiting resistance while. at lower pressure. interfacial heat transfer was as important as drop conduction.

The most important drops for heat transfer were found to be those less than ten microns in diameter. The distributions for this size range had to be inferred from the heat transfer measurements as the microscope and camera were unable to resolve drops this small.

NOMENCLATURE

A, area;
D, drop diameter;
$D_{\min}$, minimum drop diameter thermodynamically possible;
h_i, interfacial heat transfer coefficient;
h_{fg}, latent heat of vaporization;
k, liquid thermal conductivity;
m, constant;
N, number of drops in a band ± 20 per cent of D per cm^2;
$\bar{N}$, dN/dD per cm^2;
Q, rate of heat transfer;
R, resistance to heat transfer;
r, drop radius;
R_e, resistance to heat transfer due to interfacial mass transfer effects;
R_{dc}, resistance to heat transfer due to drop conduction;
R_c, resistance to heat transfer due to curvature;
t, time;
ΔT_c, temperature difference due to drop curvature;
ΔT_{dc}, temperature difference due to drop conduction;
T_s, saturation temperature;
ΔT_t, total temperature difference;
v_g, specific volume of vapor;
α, accommodation coefficient for mass transfer;
ρ_f, liquid density;
σ, surface tension.

INTRODUCTION

The RATIONAL solution of any heat transfer problem begins with the definition of the geometry. For dropwise condensation this means that the drop size distribution must be specified. The most important contribution of the present work is the measurement of the drop size distribution. In order to describe the whole drop size spectrum, it will be necessary to

use both the drop size measurements and some heat transfer measurements. These two measurements are related through theory, to be developed, for dropwise condensation. Finally the important drop size for heat transfer will be shown and the relative importance of the various heat transfer processes in dropwise condensation will be delineated.

EXPERIMENTAL PROGRAM

The same basic apparatus was used to make both the drop distribution measurements and the heat transfer measurements. A schematic of the test section is shown in Fig. 1. The test surface was a copper cylinder 0·8 in. dia. and oriented so that condensation occurred on a vertical surface. A mirror finish was used for all the measurements reported here. The polishing and promoting procedure was as follows. The surface was first polished with 0·3 and 0·05 μ aluminum oxide polishing compound and washed in distilled water. It was dipped in a 1 per cent solution of di-octadecyl disulphide dissolved in carbon tetrachloride and allowed to stand for 15 min to dry.

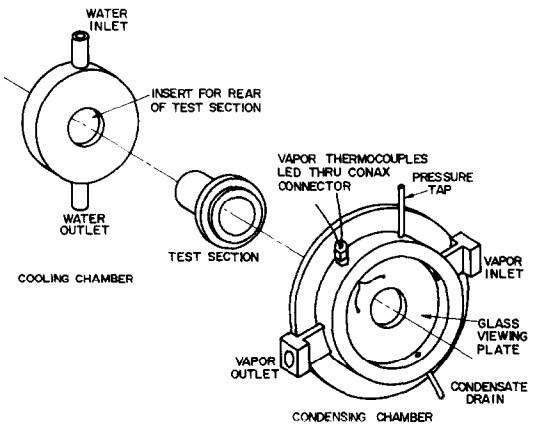

FIG. 1. Condensing chamber – test section cooling chamber assembly. The condensing surface is the disc in the front and center of the test section. It is oriented vertically.

The steam to be condensed was generated from de-gassed water. It entered at the right of Fig. 1, was partially condensed, and passed out at the left of the condensing chamber. No more than 33 per cent of the steam was condensed. The velocity of steam across the surface was low enough that the drops ran almost vertically down the test surface.

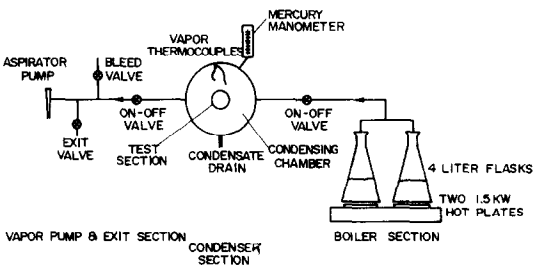

FIG. 2. Schematic layout of the vapor system.

Great care was taken both to de-gas the system and to make accurate temperature measurements. The vapor system illustrated in Fig. 2 was used to accompoish this. [1] gives the details of thermocouple placement, test section geometry, and running procedure. In general, the procedures and precautions outlined in [2] and [7] were followed both for degassing and for ensuring accurate temperature measurements. As will be clear in the section on heat transfer, the success of our attempts to minimize the temperature measurement errors and the effects of non-condensibles is indicated by the fact that the heat flux–temperature difference measurements reported here are almost the same as those reported in [2–6]. Figure 3 shows a comparison of these data with those from other sources. No direct measurements of the gas concentration in the steam were made, however.

Two separate kinds of measurements were made: heat flux and drop distributions. The relationship between the heat flux and the wall sub-cooling is shown in Fig. 4 for the two saturation temperatures which were run in these experiments.

DROP DISTRIBUTION MEASUREMENTS

A large fraction of the effort was expended in measuring the drop distributions. The actual measurements were made with a Polaroid

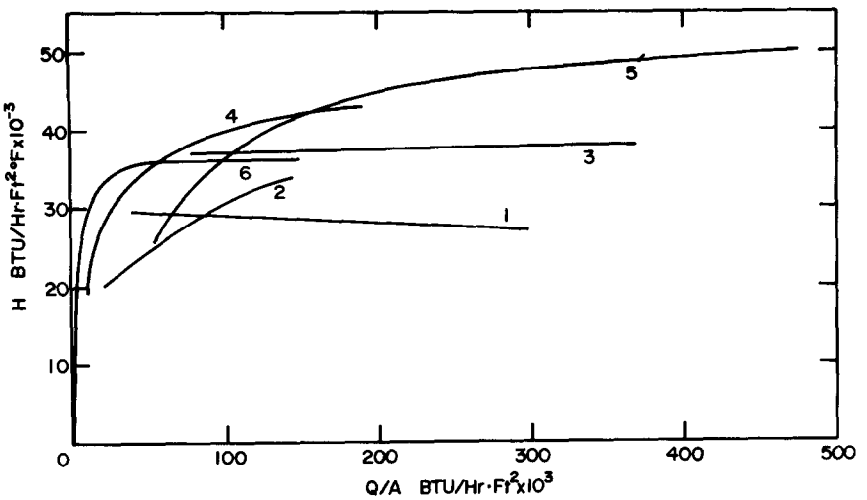

FIG. 3. Comparison of this heat transfer data with that taken by other experimenters. Perfect agreement is not to be expected as all test sections are not the same size and the venting arrangements differ. Large velocities past the surface can increase the heat transfer rate by sweeping drops off when they are still quite small.

Key: (1) Hampson and Ozisik [15]
(2) Wenzel [13]
(3) Krause [14]
(4) Tanner [6]
(5) Lefevre and Rose [4] and Citakoglu and Rose [2]
(6) Present Work

microscope camera at a variety of magnifications. The details of the procedure used to obtain these measurements are presented in [1]. Briefly, however, the procedure was as follows.

A specially constructed microscope mount was used to enable movement of the scope in both the vertical and horizontal directions. This permitted the microscope's field of view to be exactly located on the surface. Long distance objective lenses (made by Vickers) permitted high magnification (up to 400×) observation of the condensation process through the glass window. A Polaroid film pack adapted to a Leitz shutter mechanism was used for the micro-photographs.

Two types of lighting were utilized in order to get the large range of pictures needed for complete photographic coverage of the drop size spectrum. Most of the pictures were taken using a standard vertical illuminator mounted behind the objective lens. When a $\frac{1}{125}$ s shutter speed was sufficient to stop the action, an incandescent bulb was used as the light source for the illuminator. For high magnification (200× and 400×) pictures, it was necessary to use a strobe lamp of duration 10 μs placed inside the vertical illuminator to stop the action of the small "active" drops. When this technique was used, two vertical illuminators were mounted in series on the microscope. The illuminator with an incandescent bulb was used first to focus the microscope on the surface and then was shut off. The strobe illuminator could then be blinked while the shutter of the camera was open to take the picture.

The limitations of the optical system dictated the procedure which was used to take the pictures. A single picture, large enough to encompass a typical area at 400× magnification would have been ideal. However, with the film size used at 400×, the field of view was so small that one large drop filled it. Therefore a number of randomly spaced (in time) pictures at the same heat flux setting were taken. In

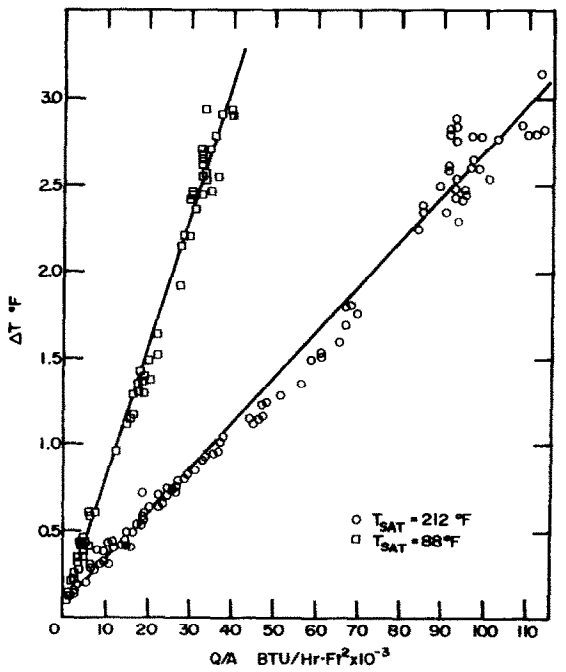

FIG. 4. Heat flux versus temperature difference curves for water vapor condensing at two different saturation temperatures on a mirror smooth copper surface. As can be seen at the left, a temperature difference of about 0·1°F is needed to get an appreciable amount of drop nucleation.

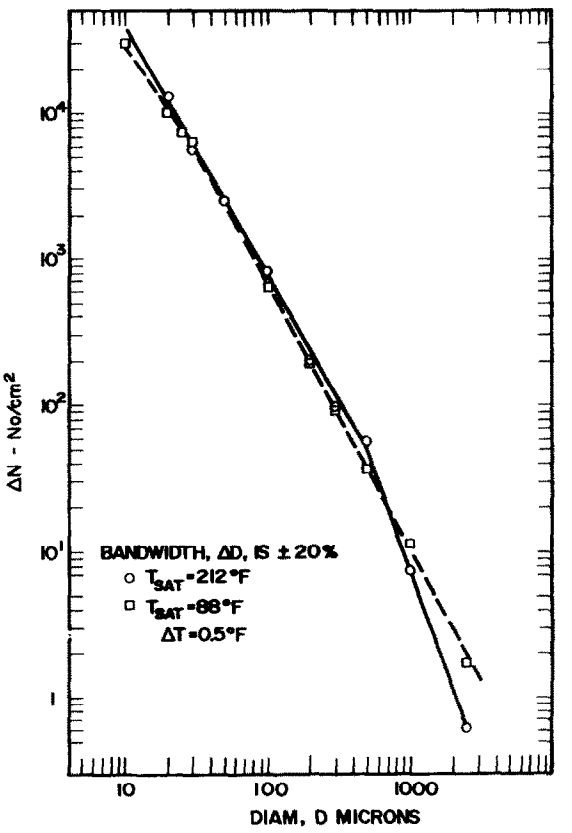

FIG. 5. Measured dropwise size distribution for a mirror smooth copper surface at two different saturation temperatures.

order to ensure a good sample it was necessary to have the number of pictures taken depend on the magnification, with more pictures necessary at higher magnifications. Reference [1], again, describes the procedure in greater detail.

Drops down to 10 μ in size were counted and measured. Drops down to one micron could be seen, but the resolution at that size was so poor that the diameter could not be determined with any accuracy. If higher magnification is used so that drops smaller than ten microns could be measured, the objective lens must be so close to the surface that it interferes with the large drops on the surface. The ten micron limit represents the lower limit for the optical system used in these experiments.

Figure 5 shows the high and low pressure drop counts. The number of drops at a given size on Fig. 5 is actually the number of drops in an average square centimeter on the surface which lie in a size range from plus to minus 20 per cent of the given size. The next section shows how the data of Fig. 5 can be used to help predict the heat transfer.

HEAT TRANSFER AND DROP POPULATION

The idea behind this section is to evaluate the heat transfer through a single drop, and then to sum the heat transfer through all the drops on the surface using the distribution given on Fig. 5. The most important assumption which must be made in order to use this procedure is that the bare spaces between the drops are completely inactive. There is no direct evidence that this is so. It is, however, not necessary to assume that any heat is transferred between the drops in order to account for all the heat transfer

observed. The possibility does exist that a two-dimensional gas is adsorbed on the surface and that it then condenses on the drops. This mechanism is not considered here.

The mechanism of dropwise condensation, as envisioned here, is as follows. Vapor condenses on the surface of the drop (through an interfacial resistance); the latent heat is conducted through the drop and thence on through the surface. It is assumed that no non-condensible gas is present. The interfacial heat transfer can be described with a heat transfer coefficient h_i in which:

$$h_i = \left[\frac{2\alpha}{2-\alpha}\right]\left(\frac{M}{2\pi R T_s}\right)^{\frac{1}{2}} \frac{H_{fg}^2}{T_s v_g}. \quad (1)$$

Equation (1) (from [8]) is, in effect, a heat transfer coefficient for mass transfer. The mass transfer accommodation coefficient, α, is taken as 1·0, as the most careful measurements appear to indicate this is what it should be for clean water.

The temperature of a drop in equilibrium with vapor at a certain pressure depends on the drop size. As the drop gets larger, the relation between the system temperature and vapor pressure approaches that of the steam tables [9]. In effect, part of the overall temperature difference driving the heat transfer is expended because of the curvature of the drops. When the Clapyron relation and the equation of equilibrium across a curved interface are combined, equation (2) results [9]:

$$\Delta T_c = \left(\frac{2T_s\sigma}{H_{fg}\rho_f}\right)\frac{1}{r}. \quad (2)$$

For a given wall subcooling, no drops below a minimum radius of curvature are possible. From equation (2), this minimum can be expressed as:

$$r_{\min} = \left(\frac{2T_s\sigma}{H_{fg}\rho_f}\right)\frac{1}{\Delta T_t}. \quad (3)$$

Forming a ratio between equations (2) and (3) allows one to express the lost temperature driving force for heat transfer due to drop curvature in a very convenient form:

$$\Delta T_c = \frac{r_{\min}}{r}\Delta T_t. \quad (4)$$

The major resistance when condensing steam is the drop conduction resistance. From [10], among others, the temperature difference due to this resistance for a hemispherical drop, is:

$$\Delta T_{dc} = \frac{Qr}{4k\pi r^2}. \quad (5)$$

If we neglect the subcooling of the liquid compared to the latent heat of condensation, the drop growth rate for a hemispherical drop is:

$$Q = \rho H_{fg} 2\pi r^2 \left(\frac{\mathrm{d}r}{\mathrm{d}t}\right). \quad (6)$$

Combining equations (1), (3) and (4), the overall temperature difference is:

$$\Delta T_t = \frac{r_{\min}}{r}\Delta T_t + \frac{Q}{h_i 2\pi r^2} + \frac{Qr}{4\pi r^2}. \quad (7)$$

When the heat transfer rate is eliminated from equation (7) by use of equation (6), and the variable is changed from radius to diameter, the result is:

$$\frac{\mathrm{d}D}{\mathrm{d}t} = \frac{4}{\rho H_{fg}}\Delta T_t\left(\frac{1 - D_{\min}/D}{D/2k + 2/h_i}\right). \quad (8)$$

This equation plus the drop size spectrum of Fig. 5 can be used to evaluate the heat transfer rate. This is accomplished by looking at the increment of heat transferred for each drop size and summing over the entire area. The result for the total heat transfer rate $(Q/A)_t$ is:

$$(Q/A)_t = \pi\Delta T_t \int_{D_{\min}}^{D_{\max}} \bar{N}D^2\left(\frac{1 - D_{\min}/D}{D/2k + 2/h_i}\right)\mathrm{d}D. \quad (9)$$

This equation can be used to predict the heat transfer on a typical surface. From the pictures, $D_{\max}$ is as follows:

Table 1

T_{sat} (°F)	D_{max} (mm)
88	3
212	2·5

$D_{\min}$ is evaluated from equation (3).

DISCUSSION AND RESULTS

The minimum drop size calculated from equation (3) turned out to be far smaller than the size measurable on the photograph even at 400 ×. Therefore, it was necessary to infer what the drop distribution was for the small sizes by integrating equation (9) for a variety of drop distributions. The right distribution was the one which gave the measured heat flux for that temperature difference. Figure 6 shows the distributions that were tried for atmospheric

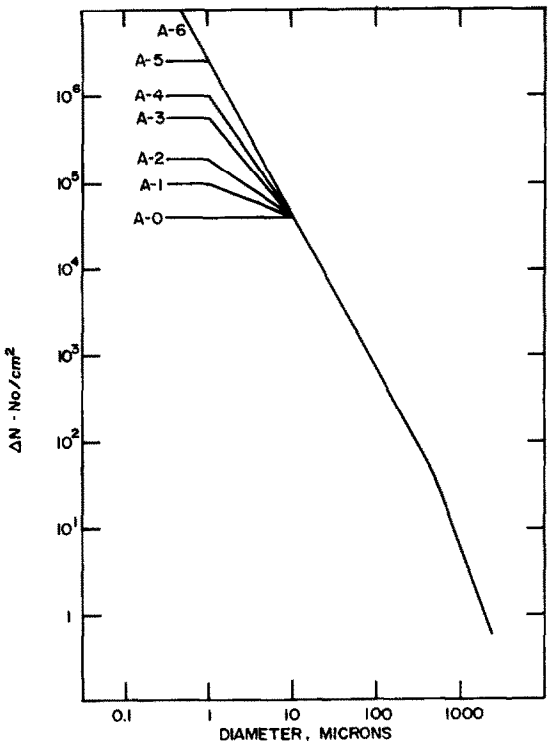

FIG. 6. Various trial drop distributions used to match the measured heat transfer data at one atmosphere pressure and measured drop distribution. Of this set, *A*-3 was the one which gave the correct heat transfer rate.

pressure condensation. The one which gave the right integrated heat transfer was chosen. A similar calculation was made for the 88°F saturation temperature heat transfer data; the resulting distribution curves for both atmospheric and low pressure are shown in Fig. 7.

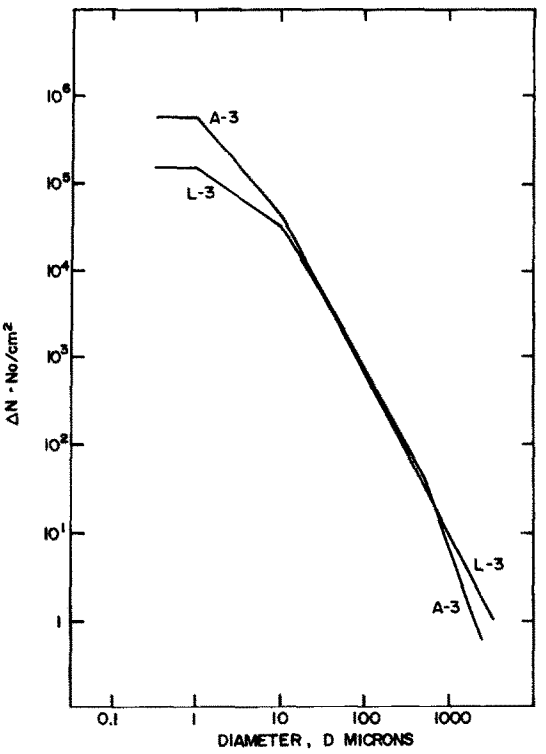

FIG. 7. The final drop distribution used in all subsequent calculations. L-3 is the low pressure (T_{sat} = 88°F) distribution curve which matched the low pressure heat transfer data in the same way that the A-3 curve matched the atmospheric pressure heat transfer data.

It is appropriate to discuss these curves, as they summarize the most important findings reported here. There are two limits which the drop populations, for drops below ten microns, must lie between. The upper limit (at one atmosphere) is line A-6 of Fig. 6. It is fixed by the agglomeration process and is determined by the statistics of drops touching when they start from a random array on the surface. [11] describes this process. The lower limit, which is clearly too low, from the photographs, assumes that only those drops which are large enough to measure are present on the surface. (There are visible drops too small to measure on the surface.) The truth lies between these limits. Unfortunately, a large proportion of the total heat is transferred by the drops which are

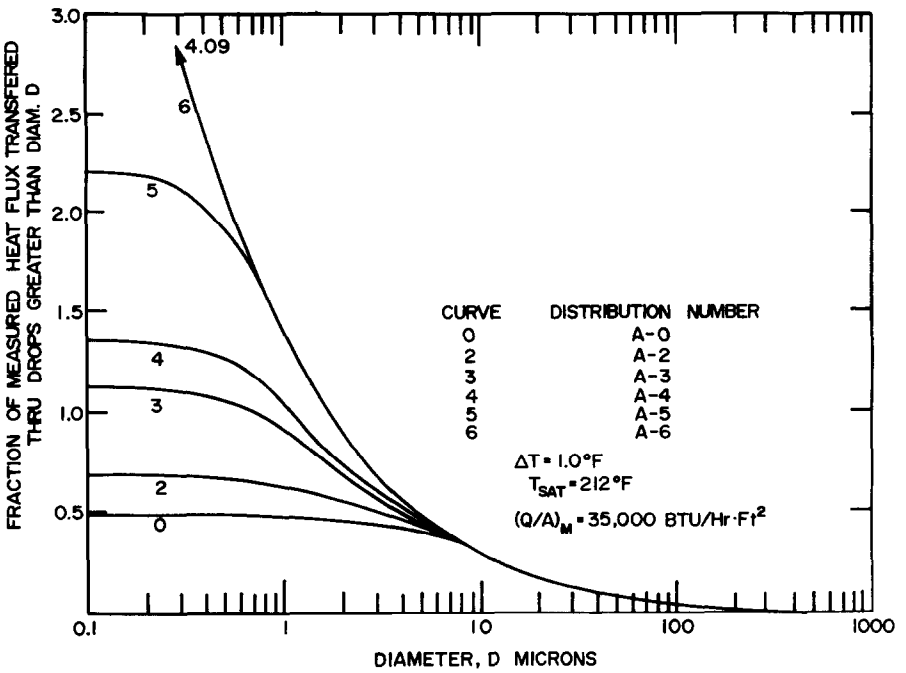

FIG. 8. The fraction of measured heat transfer which occurred in drops below the size shown. As can be seen, most of the heat is transferred in drops less than 10 μ dia. Curve 3 (the "correct" one) is slightly above 1·0 because the calculation method given in the text ignores the constriction resistance which is estimated to be about 10 per cent of the total. As can be seen for curve 3, about 60 per cent of the heat transfer is due to drops too small to measure. It is also evident that increasing the population of small drops very substantially increases the net heat transfer.

too small to measure. If we look at the limits of heat transfer, we can see on Fig. 8 how important the details of the drop distribution which is actually chosen are. Clearly the bulk of the heat transfer occurs where the drops are too small to measure.

Figure 8 shows that drop distribution A-3 gives about 12 per cent more heat transfer than is actually measured. If the constriction resistance were added into equation (9) using the theory of [12], it is estimated that the overall heat flux–temperature difference for distribution A-3 would be just about right. The details on the construction resistance are in [1] and [12]. More than 90 per cent of the heat for distribution A-3 is transferred through drops smaller than 100 μ.

A similar calculation has been completed for distribution L-3 for the data taken at a saturation temperature of 88°F. The general result is similar. It is clear that the differences between drop distributions L-3 and A-3 are large enough to be quite significant in the heat transfer. That is, if atmospheric pressure properties are used with the L-3 drop distribution the calculated heat flux will be significantly in error. This is both a surprise and a disappointment. It is a surprise because the obvious ways of changing nucleation site density, like surface roughening, have very little effect on the heat transfer [1]. Yet it is clear from Fig. 8 that changes in nucleation properties can have a large effect. Apparently at the scale in which nucleation is important the differences between various surface finishing procedures are not significant. It is a disappointment in that a simple, universal

dropwise condensation heat transfer correlation appears to be out of reach. Separate drop distribution curves will be needed for high and low pressure and for each fluid–material combination.

Figure 8 is interesting from another point of view. For all practical purposes, drops greater than 100 μ are inactive. They transfer less than 10 per cent of the total heat. If we turn to Fig. 9, curve 3, however, we can see that more than 60 per cent of the surface is covered by drops greater than 100 μ dia. When we deduct the 10 per cent bare area, we find that the remaining 30 per cent transfers 90 per cent of the heat. This is an indication of how non-uniform the heat transfer actually is on the surface.

By dropping terms out of equation (9) one by one, it is possible to see how significant the different heat transfer resistances actually are. The result of a calculation using the appropriate drop distributions is summarized on Fig. 10. It is clear that the drop conduction resistance is important at both high and low pressures.

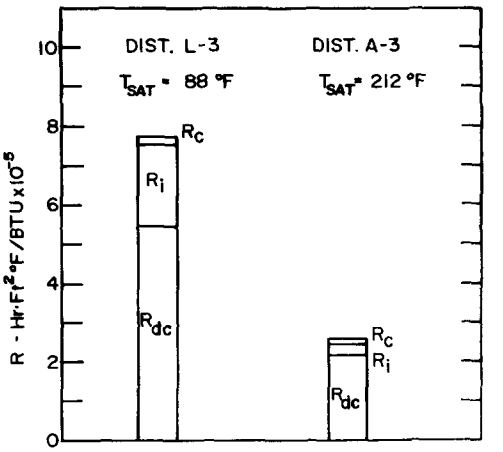

FIG. 10. The resistances to heat transfer due to the various terms in equation (9). These graphs were calculated by dropping out, one at a time, the terms in equation (9) due to interfacial resistance (that is, $h_i = \infty$), and due to curvature ($D_{min} = 0$) while leaving the other terms in. R has the units of reciprocal heat transfer coefficient. As can be seen, drop conduction is the governing resistance. In these calculations the accommodation coefficient for mass transfer has been assumed equal to 1·0.

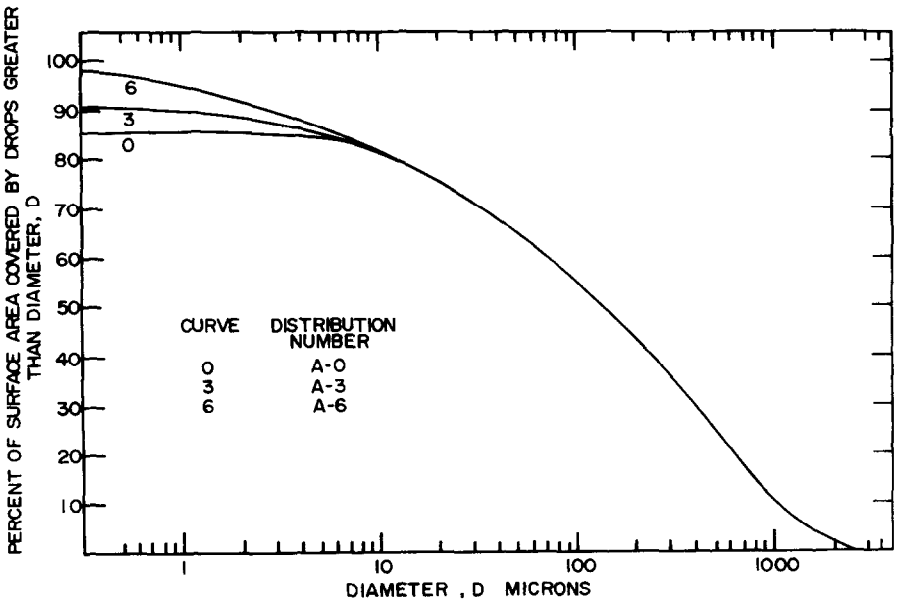

FIG. 9. Per cent of the surface covered by drops above the indicated size for distribution A-3. Curve 3 again is the "correct" one.

CONCLUSIONS

The measurements of drop distributions and the development of equation (9) allow one to compare quantitatively the various factors affecting dropwise condensation. The picture which emerges is just as complicated as the boiling picture, and just as difficult to reduce to an engineering correlation. In spite of this, our understanding of the processes which constitute dropwise condensation and of how they combine is quite good. The conclusions which we can draw from this work are summarized below.

(1) For a temperature difference of 0·5°F during low pressure condensation (T_{sat} = 88°F) the nucleation site density was measured to be 200 $\times$ 10^6 sites/cm^2. At the same temperature difference for condensation at atmospheric pressure, the site density increased by a factor of about three. Below a temperature difference of 0·5°F, the nucleation site density dropped sharply with temperature difference.

(2) For low pressure condensation (T_{sat} = 88°F) drops smaller than 150 μ dia. occupying 35 per cent of the surface area transfer 90 per cent of the total heat. At atmospheric pressure, drops of diameter less than 40 μ covering 23 per cent of the surface transfer 90 per cent of the heat. In each case, approximately 10 per cent of the surface is bare. Fifty per cent of the heat is transferred through 5 per cent of the surface area for both low and atmospheric pressure condensation.

(3) The resistance due to conduction through the drops is the most important resistance for both atmospheric and low pressure condensation.

ACKNOWLEDGEMENT

This work was entirely supported by the National Science Foundation.

REFERENCES

1. C. GRAHAM. The limiting transfer mechanisms of dropwise condensation. Ph.D. Thesis. Department of Mechanical Engineering. M.I.T. (March 1969).
2. E. CITAKOGLU and J. W. ROSE. Dropwise condensation some factors influencing the validity of heat transfer measurements, *Int. J. Heat and Mass Transfer* **11**, 523 (1968).
3. E. J. LEFEVRE and J. W. ROSE. An experimental study of heat transfer by dropwise condensation. *Int. J. Heat and Mass Transfer* **8**, 1117 (1965).
4. E. J. LEFEVRE and J. W. ROSE. A theory of heat transfer by dropwise condensation. *Proceedings of the Third International Heat Transfer Conference*. Vol. 2. p. 362 (1966).
5. J. W. ROSE. On the mechanism of dropwise condensation. *Int. J. Heat and Mass Transfer* **10**. 755 (1967).
6. D. W. TANNER, C. J. POTTER, D. POPE and D. WEST. Heat transfer in dropwise condensation. Part 1: The effects of heat flux, steam velocity, and non-condensible gas concentration. *Int. J. Heat Mass Transfer* **8**. 419 (1965).
7. S. WILCOX. Film condensation of liquid metals– precision of measurement. Ph.D. Thesis. M.I.T. (1969).
8. K. NABAVIAN and L. A. BROMLEY. Condensation coefficient of water, *Chem. Engng Sci.* **18**, 651 (1963).
9. J. H. KEENAN, *Thermodynamics*, John Wiley (1941).
10. N. FATICA and D. L. KATZ. Dropwise condensation. *Chem. Engng Prog.* **45**. 661 (1949).
11. L. R. GLICKSMAN and A. W. HUNT. Numerical simulation of dropwise condensation, *Int. J. Heat Mass Transfer* **15**, 2251–2269 (1972).
12. B. B. MIKIC. On mechanism of dropwise condensation. *Int. J. Heat Mass Transfer* **12**. 1323 (1969).
13. H. WENZEL, Versuch über Tropfenkondensation, *Allg Wärmetech*, **8**, 53 (1957).
14. J. KRAUSE, Dropwise condensation—quantitative research, Heat Division Paper No. 28, National Engineering Laboratory, East Kilbride (1950).
15. H. HAMPSON and N. OZISIK. An investigation into the condensation of steam. Institute of Mechanical Engineers. Vol. 13. 282 (1952).

DISTRIBUTION DE GOUTTES EN DIMENSION ET TRANSFERT THERMIQUE DANS UNE CONDENSATION EN GOUTTES

Résumé—Des distributions de gouttes ont été déterminées à la pression atmosphérique et à basse pression pour la condensation en gouttes du disulfure de di-octadécane sur une plaque de cuivre verticale et lisse. On a trouvé des densités de sites de nucléation proches de 200 10^6 sites/cm^2. On a constaté des populations de gouttes significativement plus grandes à la pression atmosphérique qu'aux basses pressions.

A l'aide d'une théorie de transfert thermique on a trouvé qu'à la pression atmosphérique la conduction des gouttes est la résistance limitative, tandis qu'à une pression plus basse le transfert thermique interfacial est aussi important que la conduction des gouttes.

Les gouttes les plus importantes pour le transfert thermique sont celles dont le diamètre est inférieur à dix microns. Dans ce domaine de tailles, les distributions ont été déduites des mesures de transfert thermique alors que la résolution du microscope et de la caméra était insuffisante.

DIE VERTEILUNG DER TROPFENGRÖSSE UND DER WÄRMEÜBERGANG BEI TROPFENKONDENSATION

Zusammenfassung—Die Verteilung der Tropfengrösse wurde bestimmt bei der Tropfenkondensation an einer glatten senkrechten Kupferoberfläche, die mit Dioktadecyldisulfid überzogen ist. Die Versuche wurden bei Atmosphärendruck und kleinen Drücken durchgeführt. Es wurden Keimstellendichten von $100 \cdot 10^{16}$ Keimstellen pro cm^2 gefunden. Bei Atmosphärendruck war die Tropfenhäufigkeit merklich grösser als bei niedrigeren Drücken.

Mit Hilfe der Wärmeübertragungstheorie wurde errechnet, dass bei Atmosphärendruck die Wärmeleitung im Tropfen den begrenzenden Widerstand bildet, während bei niedrigen Drücken der Wärmeübergang an der Grenzfläche gleiche Bedeutung erlangt, wie die Leitung im Tropfen. Es wurde gefunden, dass die Tropfen mit einem Durchmesser von kleiner als 10 μ bezüglich des Wärmeübergangs besonders wichtig sind. Die Verteilung der Tropfen dieser Grössenordnung musste aus den Wärmeübergangsmessungen abgeleitet werden, da das Mikroskop und die Kamera nicht in der Lage waren, Tropfen dieser Grösse aufzunehmen.

РАСПРЕДЕЛЕНИЕ КАПЕЛЬ ПО РАЗМЕРУ И ТЕПЛООБМЕН ПРИ КАПЕЛЬНОЙ КОНДЕНСАЦИИ

Аннотация—Проведено измерение распределения капель по размеру при атмосферном и пониженном давлении в процессе капельной конденсации на гладкой вертикальной поверхности из меди, активированной ди-октадецил-дисульфидом. Измеренные плотности центров конденсации равны 200×10^6 на 1 кв. см. обнаружено, что при атмосферном давлении плотность капель значительно больше, чем при пониженном.

С помощью теории теплообмена установлено, что при атмосферном давлении капельная проводимость имеет конечное сопротивление, тогда как при пониженных давлениях теплообмен на поверхности раздела играет такую же роль, как и капельная конденсация. Показано, что в процессе теплообмена большое участие принимают капли диаметром менее 10 микрон. Распределения их по размеру необходимо рассчитывать по измерениям теплообмена, т.к. наблюдения с помощью микроскопа и кинокамеры не обнаруживают таких мелких капель.